Single-Chain Conformations in Symmetric Binary Polymer Blends: Quantitative Comparison between Self-Consistent Field Calculations and Monte Carlo Simulations

M. Müller

Institut für Physik, WA 331, Johannes Gutenberg Universität, D-55099 Mainz, Germany

Received May 18, 1998; Revised Manuscript Received August 5, 1998

ABSTRACT: Single-chain properties in a symmetric binary polymer blend are studied by self-consistent field calculations and Monte Carlo simulations. Within the self-consistent field scheme, the statistical mechanics of a cluster of neighboring polymers is solved. Interactions among the polymers of a cluster and composition fluctuations within a cluster are incorporated exactly, a mean field approximation is invoked for intercluster interactions and long-range fluctuations. The results are compared to large scale Monte Carlo simulations for a broad range of chain lengths. While we find nearly quantitative agreement for single chain properties—*e.g.*, the reduction of the chain dimensions of the minority component—only qualitative agreement is achieved for thermodynamic quantities—*e.g.*, the critical temperature. The temperature and composition dependence of the chain conformations are attributed to a balance between the entropy loss upon contraction and the exchange of intermolecular and intramolecular contacts. The calculations suggest that the relative reduction of the spatial extension of the minority chains depends on the parameter $\chi\sqrt{N}$ for not too large incompatibilities χ. The scaling limit is, however, approached only for very long chain lengths N.

I. Introduction

The phase behavior and the interfacial properties of binary AB polymer blends have attracted longstanding interest. Controlling the thermodynamic properties is one key for tailoring the materials properties of composites. Hence powerful self-consistent field,[1−4] density functional,[5−7] and liquid state theories[8,9] have been developed to describe the bulk and interfacial thermodynamics of macromolecular mixtures. In addition, the influence of the particular chain architecture[10−13] on various properties has been investigated. However, the same intermolecular forces which determine the thermodynamic properties alter the conformations of the extended macromolecules. This is shown by computer simulations of a variety of models[14−19] of dense binary polymer blends. In the two-phase region chains of the minority component shrink as to reduce the number of unfavorable intermolecular interactions. The importance of the exposed surface area that makes contact with other molecular surfaces for a quantitative thermodynamic description has been realized long ago.[20,21] Electronic excitation transport measurements in a highly incompatible poly(methyl methacrylate) (PMMA) poly(vinyl acetate) (PVAc) blend of rather low molecular weight indicate a relative contraction of isolated PMMA chain extensions by 13−15%.[22] Small angle neutron scattering experiments in miscible blends report, however, only small (if any) conformational changes upon mixing.[23,24] The change of molecular dimensions is also pertinent to biological systems.[25] Computer simulations reveal ample evidence for a coupling between polymer conformation and intermolecular interaction energy: It results in a slight temperature dependence of the number of intermolecular contacts,[26] their spatial dependence across the interface between immiscible homopolymers,[26] a shrinking of symmetric AB copolymers[27] at interfaces between homopolymers, and pronounced deviations from the Flory−Huggins absorption isotherms at high incompatibilities.[28,29] The shrinking of the individual blocks and the polarization of distinct blocks (dumbbell shape) in diblock copolymer melts above the ODT have been observed experimentally[30,31] and in simulations.[32,33] Despite the ubiquitous coupling between the molecular conformation and the thermodynamic state, a thorough quantitative understanding is still lacking.

The coupling between chain conformations and intermolecular energy has been investigated in the framework of P-RISM theories,[34,35] density functional approaches,[5−7] and field-theoretic calculations.[36−40] The shrinking of the chains in the minority phase can be attributed to a balance between the entropy loss due to deviations from the ideal, unperturbed chain conformation and the energy gain upon shrinking.[28] Assuming Gaussian statistics for the single chain conformations in a melt, a deviation from the ideal unperturbed chain extension R_0 gives rise to an entropic force $(R - R_0)/R_0^2$.[41] This is opposed to an enthalpic force $\mathrm{d}E/\mathrm{d}R$, where E denotes the single chain energy as a function of the chain extension R. The energy E comprises energetically favorable interactions $N z^{\mathrm{intra}}$ among monomers of the same chain and $N z^{\mathrm{inter}}$ interactions with monomers of different polymers, where N denotes the chain length. The scale of the energy difference between AB interactions and interactions between monomers of the same type is set by the Flory−Huggins parameter χ. Similar to the situation in a dilute polymer solution,[41] the number z^{intra} of intramolecular interactions per monomer is determined by the number of pairwise contacts in the correlation hole and scales like $N z^{\mathrm{intra}} \sim N^2/\rho R_0^3$, where ρ denotes the monomer density. Under the assumption that the reduction of the chain extension does not affect the total number of interactions, but merely exchanges intermolecular interactions into energetically favorable intramolecular ones, we estimate the chain length dependence of the energy change as

10.1021/ma9807973 CCC: $15.00
Published on Web 12/01/1998

$dE/dR \sim \chi N^2/\rho R_0^4$. Balancing the entropic and enthalpic forces leads to $(R - R_0)/R_0 \sim -R_0(dE/dR)$. Hence, the relative reduction of the chain extension is proportional to $\chi N^2/\rho R_0^3 \sim \chi\sqrt{N}/\rho b^3$, where b denotes the statistical segment length. At not too high segregation, the energy scale χ of the segmental repulsion between unlike species is of the order $1/N$; thus, the relative reduction of the coil extension vanishes like $1/\sqrt{N}$. Moreover, increasing the monomer density we increase the contribution of the intermolecular interactions to the total energy. Thus changes of the single-chain conformations become increasingly inefficient in reducing the energy at high densities. If the interaction strength χ becomes comparable to $1/\sqrt{N}$, there are more pronounced changes in the chain dimensions. However, this corresponds to extremely high segregation, *i.e.*, $\chi N \sim \sqrt{N}$. These heuristic considerations are in qualitative agreement with calculations of one-loop corrections to the mean field result.[37,38] There are additional corrections to the behavior of infinite long chains, *e.g.*, the chain length dependence of the number of intermolecular contacts ("correlation hole effect") or nonrandom mixing effects which are of the same order of magnitude. While the first correction is already present in the athermal system, the second is most important close to criticality. In accord with the Ginzburg criterion[42] the ultimate long chain length behavior remains unaltered. Hence, these effects are often neglected in self-consistent field calculations in the framework of the Gaussian chain model.[1−4]

The aim of our present paper is 2-fold: First we want to introduce a numerical self-consistent field (SCF) scheme, which incorporates the detailed chain structure on all length scales and the coupling between conformation and intermolecular energy. Moreover it accounts for nonrandom mixing effects to some extent. The basic entities in our calculation are clusters of n_c neighboring polymers. Raos and Allegra[43] employed clusters of polymers to describe the structure and thermodynamics of polymer solutions. However, they neglected intercluster interactions, treated the intracluster contributions to the free energy in a mean field approximation, and used Gaussian chain conformations. While the omitting of intercluster interactions may be appropriate for dilute solutions, it is not appropriate for melts. We incorporate the coupling between intermolecular energy and conformations via an exact treatment of the intrachain energy for each polymer conformation. This is implemented via a partial enumeration scheme.[13,44−49] A similar method on a single-chain basis has been applied by Weinhold *et al.*[46] to evaluate the density dependence of the chain conformations in polymer solutions. In our scheme composition fluctuations within the cluster of polymers are treated exactly, whereas intercluster interactions are approximated by a mean field. The calculations require multichain conformations of an athermal reference system. The use of clusters of many polymers contrasts with other cluster mean field approaches by Kikuchi *et al.*[51] or Freed and co-workers,[52] which deal with clusters of many polymer segments but employ more sophisticated treatments of the intercluster free energy. We apply our scheme to a binary polymer melt and predict the phase behavior, the temperature dependence of the interactions between monomers of the same chain and different polymers, and the extension of polymers in the majority and minority phase without any adjustable parameter. The second aim of our paper is to compare the predictions of this scheme quantitatively with detailed Monte Carlo simulations of the same model. In particular, the dependence of the conformational changes on the chain length above and below the critical point is investigated for a broad range of chain lengths ($N = 16-512$) and compared to the heuristic considerations presented above. In the system under investigation, unlike species repel, and we find a shrinking of the chain extensions in the minority phase; however, in miscible mixtures with favorable interactions a chain expansion has been observed in Monte Carlo simulations.[16] We also study the phase behavior and the dependence of the effective Flory−Huggins parameter on temperature and composition. This quantitative comparison allows us to assess the validity of the approximations and assumptions invoked in our mean field treatment.

Our paper is organized as follows: In the next section we introduce the salient features of the self-consistent field scheme. It is applied to a coarse-grained polymer model, which we describe in the subsequent section. Then we present a quantitative comparison between the self-consistent calculations and our Monte Carlo results. We close with a brief discussion and an outlook on future improvements and applications. The detailed derivation of the mean field equations is deferred to the Appendix.

II. Self-Consistent Field (SCF) Model

We consider a melt comprising two polymer species denoted A and B. For simplicity, both polymer species have the same degree N of polymerization. Unlike monomers repel each other, whereas there is an attraction between monomers of the same type. We work in the semi-grand-canonical ensemble, *i.e.*, where the total number of monomers is fixed; however, the composition of the system is allowed to fluctuate, and the conjugated exchange chemical potential $\Delta\mu = \mu_A - \mu_B$ is controlled. μ_A and μ_B denote the chemical potentials of A and B polymers. In the following we outline a self-consistent field theory of multichain clusters. A multichain cluster comprises a central chain and its $n_c - 1$ neighbors. They are chosen such that the sum of the spatial distance between their centers of mass and the center of mass of the central chain is minimal. The dimensionless spatial density of A monomers belonging to the cluster α then takes the form

$$\phi_{A\alpha}(\mathbf{r}) = \frac{1}{\rho}\sum_{i_{A\alpha}=1}^{n_{A\alpha}}\sum_{s=1}^{N}\delta(\mathbf{r} - \mathbf{r}_{i_{A\alpha}}(s)) \qquad (2.1)$$

where the first sum runs over all $n_{A\alpha}$ A polymers in the cluster α and ρ denotes the monomer number density. The position of the s*th* segment of the A polymer $i_{A\alpha}$ belonging to the cluster α is denoted $\mathbf{r}_{i_{A\alpha}}(s)$. The total energy E of the system containing N_c clusters can be written in the form

$$E = -\frac{\epsilon\rho^2}{2}\sum_{\alpha,\beta}\int d\mathbf{r}\, d\mathbf{r}'\{V_{AA}(\mathbf{r}-\mathbf{r}')\hat{\phi}_{A\alpha}(\mathbf{r})\hat{\phi}_{A\alpha}(\mathbf{r}') + V_{BB}(\mathbf{r}-\mathbf{r}')\hat{\phi}_{B\alpha}(\mathbf{r})\hat{\phi}_{B\alpha}(\mathbf{r}') + V_{AB}(\mathbf{r}-\mathbf{r}')\hat{\phi}_{A\alpha}(\mathbf{r})\hat{\phi}_{B\alpha}(\mathbf{r}') + V_{AB}(\mathbf{r}-\mathbf{r}')\hat{\phi}_{B\alpha}(\mathbf{r})\hat{\phi}_{A\alpha}(\mathbf{r}')\} \qquad (2.2)$$

where V_{AA}, V_{BB}, and V_{AB} denote the pairwise interactions between the different monomer species. We de-

compose E into intercluster $E_{\alpha\beta}^{\text{inter}}$ and intracluster $E_{\alpha}^{\text{intra}}$ contributions:

$$E \equiv \sum_{\alpha} E_{\alpha}^{\text{intra}} + \sum_{\alpha \neq \beta} E_{\alpha\beta}^{\text{inter}} \tag{2.3}$$

The monomeric interactions V_{AA}, V_{BB}, and V_{AB} comprise an excluded volume (or short ranged repulsive) contribution and a weak thermal interaction. We take the thermal interactions to be of the form $\pm\epsilon\rho\nu(\mathbf{r})$, where the "+" sign holds for unlike species and the "−" sign corresponds to an attraction between monomers of the same type. ϵ sets the temperature scale of the monomeric repulsion, and ν determines the shape of the monomeric interaction potential. Let

$$c^{\text{intra}}(i,j) = \sum_{s,s'} \nu(\mathbf{r}_i(s) - \mathbf{r}_j(s')) \tag{2.4}$$

denote the strength of mutual interactions between polymers i and j in the same cluster. In the applications $\nu(\mathbf{r})$ has a square well form, and hence, we refer to $c^{\text{intra}}(i,j)$ as contacts between polymer i and j. In terms of these quantities we write the thermal contribution of the intracluster interactions in the form

$$E_{\text{therm},\alpha}^{\text{intra}} = -\frac{\epsilon}{2}\{\sum_{i_{A\alpha}j_{A\alpha}} c^{\text{intra}}(i_{A\alpha},j_{A\alpha}) + \sum_{i_{B\alpha}j_{B\alpha}} c^{\text{intra}}(i_{B\alpha},j_{B\alpha}) - \sum_{i_{A\alpha}j_{B\alpha}} c^{\text{intra}}(i_{A\alpha},j_{B\alpha}) - \sum_{i_{B\alpha}j_{A\alpha}} c^{\text{intra}}(i_{B\alpha},j_{A\alpha})\} \tag{2.5}$$

where the sum $i_{A\alpha}$ runs over all A polymers in the cluster α. The thermal intercluster interaction takes the form

$$E_{\text{therm},\alpha\beta}^{\text{inter}} = -\frac{\epsilon\rho^2}{2}\int \mathrm{d}\mathbf{r}\, \mathrm{d}\mathbf{r}'\, \nu(\mathbf{r}-\mathbf{r}')\{\hat{\phi}_{A\alpha}(\mathbf{r})\hat{\phi}_{A\alpha}(\mathbf{r}') + \hat{\phi}_{B\alpha}(\mathbf{r})\hat{\phi}_{B\alpha}(\mathbf{r}') - \hat{\phi}_{A\alpha}(\mathbf{r})\hat{\phi}_{B\alpha}(\mathbf{r}') - \hat{\phi}_{B\alpha}(\mathbf{r})\hat{\phi}_{A\alpha}(\mathbf{r}')\} \tag{2.6}$$

For simplicity we assume the excluded volume to be the same for both monomer species. Let P denote the statistical weight of a multichain conformation in an athermal (*i.e.*, only excluded volume interactions are operative) melt. These conformations fullfill the intracluster excluded volume constraint. The intercluster excluded volume interaction in the thermal melt can be treated only approximately. In a constant volume ensemble, we assume that these interactions constrain the intercluster excluded volume to a constant value; *i.e.*, the weak thermal interactions do not shift the intercluster excluded volume away from its value in the athermal melt. The insensitivity of the fluid structure in a melt with respect to weak thermal interactions has been verified in Monte Carlo simulations of lattice models[53] and continuous space models.[7] However, this assumption has to be used with caution in strongly attractive systems, where there are pronounced changes in the fluid structure in the vicinity of the Θ temperature, below which there is a phase separation into two phases of different polymer density. For long chain lengths and meltlike densities, however, the temperature of the AB demixing transition increases linearly with chain length while the Θ temperature is chain length independent. Hence, both temperature scales are well separated for long chains. Moreover, at lower monomer densities, *i.e.*, in ternary solutions of two polymers and a solvent, excluded volume effects become more important and a much richer behavior is anticipated.[54−56]

To make progress we take the value of the intercluster excluded volume to be proportional to the number of intercluster contacts c^{inter}. The spatial density of intercluster contacts can be written in the form

$$c^{\text{inter}}(\mathbf{r}) = \frac{1}{2}\sum_{\gamma} c_{\gamma}^{\text{inter}}(\mathbf{r}) \quad \text{with}$$
$$c_{\gamma}^{\text{inter}}(\mathbf{r}) = \sum_{\beta'}\rho\int \mathrm{d}\mathbf{r}'\, \nu(\mathbf{r}-\mathbf{r}')[\hat{\phi}_{A\gamma}(\mathbf{r}) + \hat{\phi}_{B\gamma}(\mathbf{r})][\hat{\phi}_{A\beta}(\mathbf{r}') + \hat{\phi}_{B\beta}(\mathbf{r}')] \tag{2.7}$$

where the primed sum β' runs over all clusters except the cluster γ itself. For large clusters, it is small at the center of the cluster and the major contributions come from the cluster's surface. This approximation of the intercluster excluded volume is certainly a crude one, but it is physically intuitive, if the range of the thermal interactions is comparable to the spatial extent of the first neighbor shell in the monomer−monomer density pair correlation function. This assumption holds for the model studied numerically in the next section. We could certainly improve the latter estimate for the exposed surface area of a cluster by estimating the volume not accessible to chains of different clusters for each multichain conformation in the spirit of generalized Flory−Huggins theories.[57] However, this procedure would entail more model dependent information, and we shall see by comparing the predictions of our SCF theory to the simulation results that this rather crude estimate of the intercluster excluded volume describes the system satisfactorily.

In the limit that the multichain conformation is reduced to a single threadlike chain the number of intercluster contacts is proportional to the monomer density and the constraint is equivalent to the well-known incompressibility condition. In this case (cf. Appendix) we also recover the Flory−Huggins expression for the free energy. In the limit of very large multichain conformations, the clusters are compact and the intracluster interactions dominate the behavior completely. The intercluster interactions are merely surface effects and can, hence, be disregarded.[43] Our treatment of the intercluster interactions describes both limits appropriately.

In summary, we take the semi-grand-canonical partition function of the multichain system to be

$$Z(T,\Delta\mu) \sim \int \Pi_{\alpha} D_{\alpha}[\mathbf{r}] P_{\alpha}[\mathbf{r}] \times \exp\left(\frac{-\sum_{\alpha} E_{\text{therm}\alpha}^{\text{intra}}}{k_{\text{B}}T} \frac{-\sum_{\alpha\neq\beta} E_{\text{therm}\alpha\beta}^{\text{inter}} \Delta\mu \sum_{\alpha} n_{A\alpha}}{k_{\text{B}}T}\right) \times \delta(c^{\text{inter}}(\mathbf{r}) - c_{\text{atherm}}^{\text{inter}}) \tag{2.8}$$

D_{α} sums over all chain conformations and identities (*i.e.*, A or B) in the cluster α. E_{therm} denotes the thermal monomeric interaction, $\Delta\mu$ represents the exchange potential between A and B polymers, and $c_{\text{atherm}}^{\text{inter}}$ denotes the intercluster contact density in the athermal melt (*i.e.*, the reference system).

In the Appendix we formally derive the self-consistent field equations for a multichain cluster system. The

composition of the spatially homogeneous system $\bar{\phi}_A$ is given by the average over multichain conformations γ

$$\bar{\phi}_A = 1 - \bar{\phi}_B = \frac{N_c}{V}\int d\mathbf{r}\, \phi_A(\mathbf{r}) = \frac{N}{\rho V}\sum_{\gamma=1}^{N_c}\langle n_{A\gamma}\rangle = \frac{1}{n_c}\frac{\int DP\omega_\gamma n_{A\gamma}}{\int DP\omega_\gamma} \quad (2.9)$$

with respect to the cluster Boltzmann weight ω_γ. $N_c = \rho V/Nn_A$ denotes the number of clusters in the system of volume V. Short ranged fluctuations are partially incorporated into our treatment *via* an explicit enumeration of all combination of chain identities—A or B—within the cluster, whereas long-range fluctuations are ignored. The weight takes the form

$$\omega_\gamma = \exp\left(-\frac{E^{intra}_{therm\gamma}}{k_BT} + \frac{\epsilon}{k_BT}(\bar{\phi}_A - \bar{\phi}_B)[\sum_{i_{A\gamma}=1}^{n_{A\gamma}} c^{inter}(i_{A\gamma}) - \sum_{i_{B\gamma}=1}^{n_{B\gamma}} c^{inter}(i_{B\gamma})] + \pi\sum_{i_\gamma=1}^{n_c} c^{inter}(i_\gamma) + \frac{\Delta\mu n_{A\gamma}}{k_BT}\right) \quad (2.10)$$

The first term describes the pairwise thermal interactions inside the cluster according to eq 2.5. Intracluster interactions are treated exactly while intercluster interactions are replaced by fields of mean potentials which are characteristic for a local environment of composition $\bar{\phi}_A$. The second term is the mean field expression for the thermal intercluster interactions. The intercluster contacts of polymer i_γ

$$c^{inter}(i_\gamma) = \sum_{s=1}^{N}\sum_{\beta'}\rho\int d\mathbf{r}'\, v(\mathbf{r}_{i\gamma}(s) - \mathbf{r}')[\phi_{A\beta}(\mathbf{r}') + \phi_{B\beta}(\mathbf{r}')] \quad (2.11)$$

are related to the fluidlike structure of the dense athermal melt. The intercluster excluded volume interactions constrain the number of intercluster contacts and the intercluster packing interaction π has to be adjusted such that

$$\frac{\int DP\omega_\gamma\sum_{i_\gamma=1}^{n_c} c^{inter}(i_\gamma)}{\int DP\omega_\gamma} = \text{const} \quad (2.12)$$

attains its value in the athermal melt. In the third term of the cluster Boltzmann weight $\Delta\mu$ denotes the exchange potential between the different polymer species.

Equations 2.9, 2.10, and 2.12 constitute the complete set of SCF equations for a homogeneous system. These equations describe the thermodynamics of a multichain cluster placed into a potential of mean field, which in turn is determined self-consistently by the average composition of the cluster. We perform the average over the single cluster properties via a partial enumeration scheme.[13,44−49] The conformational integral $\int DP$ is approximated by a summation over a large, representative number of multichain conformations extracted from a Monte Carlo simulation of the reference system (*i.e.*, athermal melts) and all possible combinations of chain identities (A or B) of the polymers in a cluster. We would like to emphasize that the computational effort of this SCF scheme is 2 orders of magnitude smaller than the one invested in the detailed Monte Carlo simulations described in the following section.

III. The Bond Fluctuation Model: Single-Chain and Cluster Properties

In the following we apply the SCF scheme to the bond fluctuation model[58] and compare its predictions quantitatively with Monte Carlo simulations. This coarse-grained lattice model combines the computational tractability with important qualitative features of real polymeric materials: monomer excluded volume, connectivity of monomers along the polymer and a short ranged thermal interaction between monomeric units. Within the framework of this model, each monomer blocks a whole unit cell of a simple cubic lattice from further occupation. Monomers along a chain are connected via bond vectors of length 2, $\sqrt{5}$, $\sqrt{6}$, 3, and $\sqrt{10}$ lattice spacings. In the following all lengths are measured in units of the lattice spacing. The blend comprises two structurally symmetric polymer species—A and B—of the same chain length N = 16, 32, 64, 128, 256, or 512. Thermal binary monomer interactions are catered for by a short-range square well potential: $v(\mathbf{r}) = 1$ for $r \le \sqrt{6}$ and 0 otherwise. Consequentially, the potential extends over those 54 neighboring lattice sites that contribute to the first peak of the radial density correlation function. The contact of monomers of the same type lowers the energy by ϵ, whereas contacts between unlike species increase the energy by the same amount. Though our SCFT scheme is applicable to arbitrary models of extended molecules, we have chosen the bond fluctuation model because many configurational properties of the model have been previously determined.[59] Additionally the critical point behavior of this lattice model has been studied via large scale Monte Carlo simulations by Deutsch and Binder.[17] Using a finite size crossover scaling analysis, they obtained accurate estimates of the critical temperatures for chain lengths N = 16−256. In the present study we complement these results with the measurement of the chain extensions of the minority component for various temperatures below the critical temperatures, which range from the weak segregation limit to rather strong segregation.

We perform simulations in the semi-grand-canonical ensemble, *i.e.*, at fixed temperature k_BT/ϵ and exchange potential $\Delta\mu/k_BT$. By virtue of the symmetry with respect to the exchange of labels A ⇌ B, phase coexistence occurs at $\Delta\mu = 0$. The Monte Carlo procedure comprises two kind of movements: Canonical moves evolve the conformations of the macromolecules but leave the composition of the system unaltered. We employ a combination of local monomer hops and slithering snake movements. The latter relax the chain conformations a factor N faster than the local monomer hops. The semi-grand-canonical moves consist of an exchange of the polymer label A *vs* B. We employ the different Monte Carlo moves in the ratio local hopping: slithering snake:semi-grand-canonical = 4:12:1, which are chosen as to relax the conformational properties and the composition fluctuations on similar time scales.

We simulate a cubic system of lateral extension $L = 80 \approx 4R_g(N = 256)$ and apply periodic boundary conditions in all spatial directions. Some additional data for chain length N = 512 and L = 128 have been generated. Our monomer density ρ = 0.5/8 corresponds to a concentrated solution or a melt. The screening length

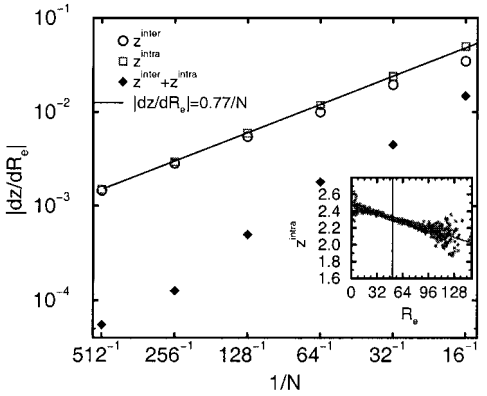

Figure 1. Correlation between the athermal polymer extension and the number of inter and intramolecular contacts per monomer on a double logarithmic scale. The straight line presents the expected $1/N$ dependence. Filled diamonds mark the dependence of the total number of contacts. The inset presents the number of intrachain contacts z^{intra} as a function of the end-to-end distance for the chain length $N = 256$ and $\epsilon = 0$. The vertical line marks the average end-to-end distance R_e in an athermal melt.

of the excluded volume interaction above which the chain conformations exhibit Gaussian statistics is about 6 lattice spacings[59] at this density, which is comparable to the chain extensions for small chain lengths ($R_g(N = 32) \approx 7$).

Upon increasing the chain length N, we reduce the intermolecular contacts of a given monomer and increase the intramolecular contacts in turn. This correlation hole effect results in a chain length dependence of the number of intermolecular contacts z^{inter} per monomer. For the athermal system[53] ($\epsilon = 0$) the measurement of the intermolecular pair correlation function yields $z^{inter}_{atherm} = 2.10(1) + 2.80(6)/\sqrt{N}$. Similarly one finds that by increasing the chain stiffness[13,60] and thereby increasing the chain extension, we can also increase the number of intermolecular contacts. As noted in the introduction the number of intramolecular contacts depends on the instantaneous shape of the polymer. In the inset of Figure 1 we present the number of intramolecular contacts z^{intra} per monomer as a function of the instantaneous end-to-end distance R_e for chain length $N = 256$. We estimate the correlation between the instantaneous chain extension and the number of intermolecular contacts z^{intra} at fixed chain length by measuring the slope of the curve $|dz/dR_e|$ at the average chain extension $\sqrt{\langle R_e^2 \rangle}$ and at fixed chain length.[61] This value is indicated as a vertical line in the inset. However, if we used the radius of gyration instead of the end-to-end distance (not shown), we would find a much smaller region of linear correlation between the number of contacts and the radius of gyration. Hence, we anticipate a rather slow approach of the long chain length scaling limit.

Since the number of intramolecular contacts scales like $z^{intra} \sim N/R_e^3$ the slope $|dz/dR_e|$ is expected to vanish like $1/N$. Indeed, this is confirmed by our Monte Carlo results in Figure 1, both for the number of intramolecular z^{intra} and intermolecular z^{inter} contacts. From this figure we estimate $|dz/dR_e| = 0.77(7)/N$ for long chains. If the conformational changes merely resulted in an exchange of inter- and intramolecular contacts both correlations would have the same absolute value (and opposite sign). This, however, is only fulfilled for the largest chain lengths, whereas there are some deviations for the smaller ones. The sum of inter- and intramolecular contacts does depend on the chain extension; however, the dependence is smaller and decays faster with growing chain length than the correlation for the intramolecular contacts. This indicates again a rather gradual approach to the large chain length scaling behavior. Moreover, the total number of contacts is also slightly temperature dependent. At strong segregation the concentration of the minority component is vanishingly small, and the system can only lower its energy by increasing the number of contacts. Hence the total number of contacts per monomer slightly increases upon lowering the temperature. This effect is not captured by the SCF calculations. However, it only becomes important on a temperature scale comparable to the Θ temperature.

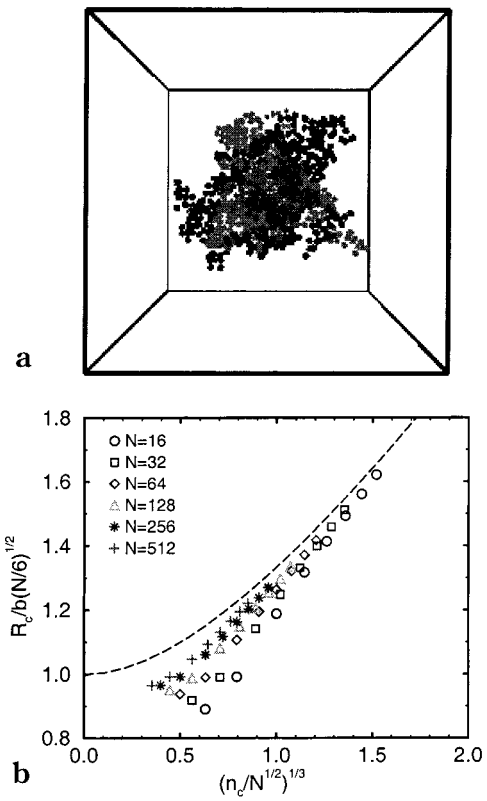

Figure 2. (a) Typical conformation of a cluster, comprising $n_c = 10$ chains of length $N = 128$. The size of the simulation cell ($L = 80$) from which we extract the cluster conformations is indicated by a frame. (b) Scaling of the cluster radius of gyration R_c with the number of chains n_c in a cluster and their chain length N. $b(N/6)^{1/2}$ measures the single chain radius of gyration. Units are chosen such that the extension of large compact clusters correspond to a straight line. The dashed line is only an illustration of the limiting long chain length behavior.

From Monte Carlo simulations of the athermal system we extract cluster configurations, which we then employ in the SCF calculations. A typical snapshot of a cluster conformation ($N = 128$, $n_c = 10$) is presented in Figure 2. For large number of chains n_c in the cluster and small chain length N, the clusters are compact; hence, the cluster extension scales as $R_c^3 \sim n_c N$. In the opposite case, the extension of the cluster is dominated by the single chain extension $R_c \sim N^{1/2}$. The scaling of the cluster size, as measured by its radius of gyration R_c, is presented in Figure 2b. It does not work particularly well for small n_c, because the average distance between chains, which scales as $(N/\rho)^{1/3}$, constitutes a second (not

dominant) length scale of the cluster extension. Note that for the clusters employed in the present study, the extension is never large compared to the single chain's radius of gyration $R_g \approx b\sqrt{N/6}$. Here, $b \approx 3.3(1)$ denotes the statistical segment length in the limit of long chain lengths. Even a cluster comprising $n_c = 14$ polymers of length $N = 16$ exceeds the single chain radius of gyration only by a factor 1.7. Thus the clusters investigated are not compact and intercluster interactions are not negligible. This is also evident from the snapshot (cf. Figure 2a). Consequentially, the mean fields which represent the intercluster interactions are important for the cluster sizes studied here. We do not attempt a systematic finite size scaling with the cluster size n_c, because our data are just in the crossover region toward compact clusters and span only a very modest regime of cluster sizes.

IV. Results

In this section we present applications of our SCF calculations to a variety of conformational and thermodynamic properties in the one-phase and two-phase regions. We compare these results to Monte Carlo simulations without any adjustable parameter.

According to the Flory−Huggins theory[62] a binary polymer blend exhibits an upper critical solution point (UCSP). Below this critical temperature, the system phase separates into an A-rich and B-rich phases. For a single threadlike chain, our SCF scheme reduces to the Flory−Huggins theory. In the following we use the intermolecular pair correlation function—as measured in Monte Carlo simulations[53]—to determine the number of contacts $z^{\text{inter}}_{\text{atherm}}$ per monomer of the athermal system, to estimate the Flory−Huggins parameter according to $\chi = 2\epsilon z^{\text{inter}}_{\text{atherm}}/k_BT$[53], and to calculate the predictions of the Flory−Huggins theory. If we used the total number of contacts (and not just the number of intermolecular contacts) as suggest by the original Flory−Huggins theory, the critical temperature in the long chain length limit would be overestimated by the mean field theory. Due to this correlation hole effect of the athermal system χ parameters differ by more than 20% for different chain lengths ($N = 16-512$) but equal monomeric interaction strength ϵ. However, this identification of the Flory−Huggins parameter does not capture the effect of conformational changes or composition fluctuations. In the long chain length limit, the polymers strongly interdigitate and interact with many neighbors. Hence, composition fluctuations are strongly suppressed in accord with the Ginzburg criterion,[42] and also conformational changes become less important. Therefore the Flory−Huggins theory becomes an appropriate description of the long chain length limit. This has been confirmed by Monte Carlo simulations.[53]

The simulations indicate, however, that there are corrections to the mean field estimate for the critical temperature of relative order $1/\sqrt{N}$: Nonrandom mixing effects in the vicinity of the critical point impart corrections on the order of $\epsilon\sqrt{N} \sim 1/\sqrt{N}$. The scaling of these nonrandom mixing effects with the chain length is in agreement with P-RISM[63] and field-theoretical calculations.[37,38] The coupling between chain conformations and intermolecular energy gives rise to an additional free energy contribution which depends *via* the same combination $\epsilon\sqrt{N}$ on chain length and interaction energy.

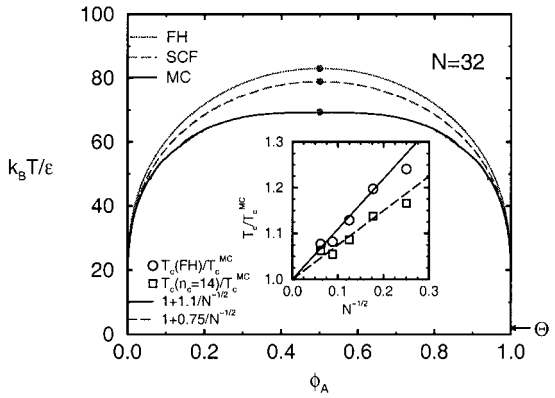

Figure 3. Phase diagram for chain length $N = 32$. The upper curve is the prediction of the Flory−Huggins theory. The dashed curve is the result of our SCF calculations with cluster size $n_c = 12$. The lower binodal presents the Monte Carlo results. The arrow at the right hand side marks the Θ-point ($\epsilon_\Theta/k_BT = 0.495$), where isolated chains collapse. The inset shows the relative overestimation of the critical temperature by the mean field theory. The circles correspond to the Flory−Huggins theory; squares denote the results of the SCF for cluster size $n_c = 14$. The straight lines show the expected $1/N^{1/2}$ dependence. Using cluster size $n_c = 14$ instead of the Flory−Huggins theory we can reduce the relative deviation between the mean field and the Monte Carlo results by one-third.

The phase diagram of a binary polymer blend of chain length $N = 32$ is presented in Figure 3. The upper curve is the prediction of the Flory−Huggins theory, the dashed line presents the results of our SCF with cluster size $n_c = 12$, whereas the lower curve corresponds to the finite size scaling analysis of Monte Carlo simulations. Of course, both mean field theories overestimate the critical temperature and cannot reproduce the flat binodals close to the critical point. The latter is the indication of the Ising universality class, which dominates the entire critical behavior for the short chain length $N = 32$. Note, however, that the SCF calculation yields an improved estimate for the binodal. This is investigated in detail in the inset of Figure 3. The relative deviation of the mean field estimate for the critical temperature and the "exact" Monte Carlo result decreases like $1/\sqrt{N}$ with growing chain length. The effective amplitude of the deviation for cluster size $n_c = 14$ is reduced by one-third in comparison with the Flory−Huggins estimate. The larger the cluster size the more composition fluctuations are incorporated. However, for the cluster sizes used in the present study the clusters are not much larger than the chain extension, and hence, we obtain only a modest improvement for the estimate of the critical temperature.

Prior Monte Carlo simulations[14,15,15] reveal that the single-chain conformations in a binary blend depend on the temperature. This effect is in contrast to the Flory−Huggins theory, which does not predict any conformational changes upon varying the temperature or composition of the blend. The temperature dependence of the end-to-end distance at $\bar{\phi}_A = 0.5$ above the critical temperature is presented in Figure 4. The chain conformations shrink upon approaching the critical temperature and the magnitude of the effect decreases upon increasing the chain length. The SCF calculations and the Monte Carlo simulations agree nicely for the shortest chains ($N = 16$),[18] where the shrinking is most pronounced.

In the pure phases all contacts are energetically favorable and the chains are more extended than in the

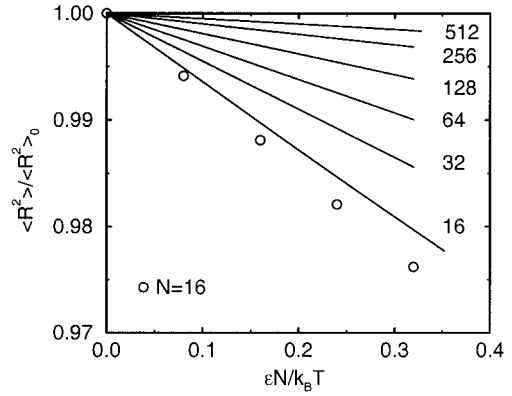

Figure 4. Temperature and chain length dependence of the end-to-end distance at $\bar{\phi}_A$. The lines present the results of the SCF calculations ($n_c = 14$) for chain length $N = 16$, 32, 64, 128, 256, and 512 (from bottom to top), while the symbols display the results of a Monte Carlo simulation for chain length $N = 16$.

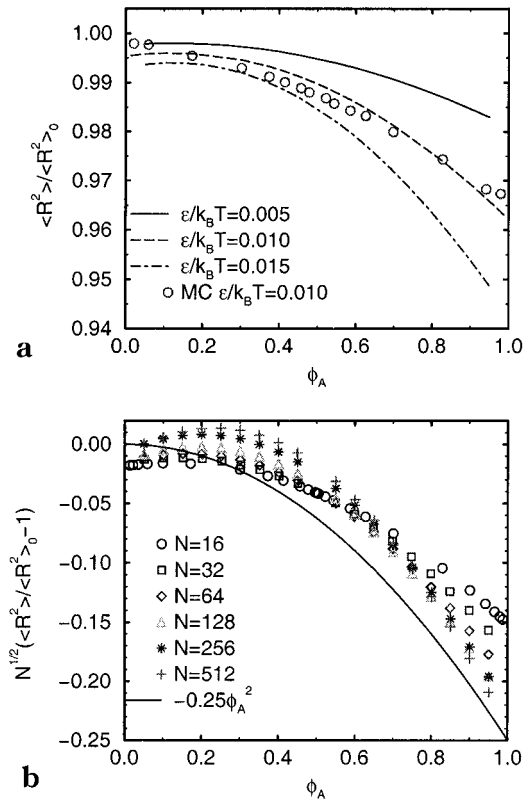

Figure 5. Composition dependence of the B chain conformations: (a) Results of the SCF for chain length $N = 16$ in the one phase region are indicated by lines. The symbols correspond to the MC simulations at $\epsilon/k_BT = 0.010$. (b) Composition dependence of the chain extensions for chain length $N = 16$, 32, 64, 128, 256, and 512 at fixed $\epsilon N/k_BT = 0.16$. Symbols correspond to the SCF calculations, whereas the solid line marks the simple estimate for the asymptotic behavior.

mixed system ($\bar{\phi}_A = 0.5$). For chain length $N = 16$, the squared end-to-end distance of the minority component shrinks about 5%. Figure 5a shows that the deviation form the unperturbed chain dimension depends roughly quadratically on the composition (see below). The SCF calculations and the Monte Carlo results for $\epsilon = 0.01$ k_BT agree gratifyingly. The SCF calculations show that the effect increases at higher incompatibilities. Moreover, the longer the chain length the weaker the composition dependence of the chain dimensions at constant ϵN. This chain length dependency in the SCF calculations is studied in Figure 5b.

The qualitative temperature and chain length behavior is in agreement with the heuristic considerations presented in the introduction. Let $P(R)$ denote the single chain probability distribution which incorporates the correlation between the chain extension and the energy E; *i.e.*, $E(R) \approx E(\sqrt{\langle R_e^2\rangle_0}) + dE/dR(|R| - \sqrt{\langle R_e^2\rangle_0})$. Assuming Gaussian statistics for the unperturbed chain, we can write the mean squared end-to-end distance in the form

$$\langle R_e^2\rangle = \frac{\int d^3\mathbf{R}\, P(R) R^2}{\int d^3\mathbf{R}\, P(R)} \quad \text{with}$$

$$P(R) \sim \exp\left(-\frac{3R^2}{2\langle R_e^2\rangle_0}\right) \exp\left(-\frac{dE}{dR}(|R| - \sqrt{\langle R_e^2\rangle_0})\right)$$

$$\langle R_e^2\rangle \approx \langle R_e^2\rangle_0 \left(1 - \sqrt{\frac{8}{27\pi}} \frac{dE}{dR} \sqrt{\langle R_e^2\rangle_0}\right) \tag{4.1}$$

where $\langle R_e^2\rangle_0 = b^2 N$ denotes the unperturbed squared end-to-end distance. We have assumed that dE/dR $\sqrt{\langle R_e^2\rangle_0}$ is small. The total energy change associated with the transfer of two intermolecular contacts of a B polymer $[\epsilon(\bar{\phi}_A - \bar{\phi}_B)]$ into an intramolecular contact $[-\epsilon]$ and a contact between monomers not belonging to this B polymer $[-\epsilon(\bar{\phi}_A - \bar{\phi}_B)^2]$ amounts to $\Delta E = 4\epsilon\phi_A^2$. The number of intramolecular contacts per monomer increases by 2, and the number of intermolecular contacts decreases by the same amount. Hence, we obtain for the composition and temperature dependence of the extension of a B polymer

$$\langle R_e^2\rangle = \langle R_e^2\rangle_0 \left(1 - 2\sqrt{\frac{8}{27\pi}} \frac{b}{\sqrt{N}} \left(\frac{dz}{dR} N\right) \epsilon N \bar{\phi}_A^2\right) \tag{4.2}$$

We expect this asymptotic expression to hold only for very small values of $\epsilon\sqrt{N}$ (see below).[50] However, this simple estimate rationalizes the quadratic composition dependence and the temperature and chain length variation. The corresponding prediction is presented in Figure 5b as a solid line. It agrees reasonably well with the long chain length behavior of the SCF calculations. At present, however, we cannot offer an explanation for the maximum of the curves around $\bar{\phi}_A \approx 0.2$ and long chain lengths. For chain length $N = 256$ a deviation of 0.02 on the scale of Figure 5b corresponds to a relative accuracy of the mean end-to-end distance of 0.001. This is comparable to or even smaller than the statistical accuracy of the finite sample of conformations employed in the SCF calculations.

As the conformational entropy loss due to chain shrinking is balanced against the exchange of inter- and intramolecular contacts, the macromolecules reduce their free energy. Hence, we expect that the composition dependence of the chain dimensions above the critical temperature gives rise to a slight composition dependence of the effective Flory−Huggins parameter. We define an effective χ_{FH} *via* the semi-grand-canonical equation of state (cf. Appendix, eq 5.12):

$$\chi_{FH} \equiv -\frac{\Delta\mu/k_BT - \ln(\bar{\phi}_A/(1-\bar{\phi}_A))}{(2\bar{\phi}_A - 1)N} \tag{4.3}$$

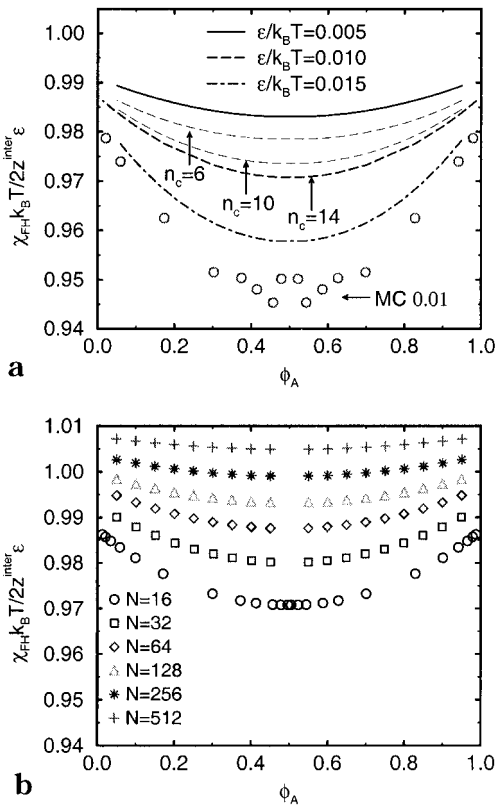

Figure 6. Composition dependence of the effective Flory−Huggins parameter in the one phase region: (a) Results of the SCF calculation ($n_c = 14$) for chain length $N = 16$. Results for small cluster size for $\epsilon/k_BT = 0.01$ are indicated by thin dashed lines. The symbols display the results of the MC simulations at $\epsilon = 0.010$. (b) Composition dependence of the Flory−Huggins parameter for chain length $N = 16$, 32, 64, 128, 256, and 512 from bottom to top at fixed $\epsilon N/k_BT = 0.16$.

The equation of state which relates the composition $\bar{\phi}_A$ of the mixture to the exchange potential $\Delta\mu$ is immediately accessible in the Monte Carlo simulations[60] in the semi-grand-canonical ensemble and establishes a direct link between the Monte Carlo simulations and the thermodynamics of the blend. The composition dependence of the effective Flory−Huggins parameter is shown in Figure 6a. The SCF calculations exhibit a small upward parabolic dependence of χ_{FH} on the composition. The composition dependence is the larger the stronger the incompatibility. The results of the Monte Carlo simulations are presented as symbols in Figure 6a. Unfortunately the simulation results exhibit quite some scatter, especially around $\bar{\phi}_A$ due to the denominator in the above equation. The comparison shows that the effect is only qualitatively captured by the SCF calculations; the Monte Carlo simulations exhibit a stronger dependence on the composition. One reason for this discrepancy is composition fluctuations which are incorporated into the mean field calculations only to a very limited extent. Increasing the cluster size (n_c = 6, 10, 14), we incorporate more composition fluctuations in our mean field calculations; the composition dependence increases and the SCF results get closer to the Monte Carlo data. However, for the cluster sizes available, we do not achieve quantitative agreement. In the framework of the SCF calculations an increase of the chain length results into a smaller composition dependence of the effective Flory−Huggins parameter at constant ϵN. This is investigated in Figure 6b. Note

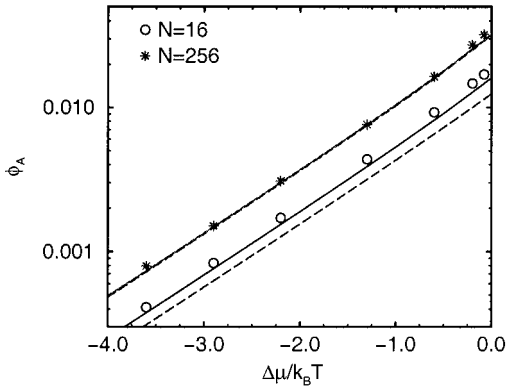

Figure 7. Absorption isotherms for chain lengths $N = 16$ and $N = 256$ at $\epsilon N = 0.8$. The symbols are the result of the Monte Carlo simulations, the solid lines presents the results of our SCF calculation ($n_c = 14$) and the dashed lines corresponds to the Flory−Huggins estimate.

that values of $\chi_{FH} > 1$ are due to uncertainties of the estimate for z^{inter}_{atherm} in the athermal system, which are about 1%. A similar upward parabolic composition dependence of the effective Flory−Huggins parameter has been seen in prior Monte Carlo simulations[14] and it is qualitatively in agreement with calculations of Garas and Kosmas.[38]

Further below the critical temperature, the correlation length of composition fluctuations is of the coil size and conformational changes become more important. Indeed, the Flory−Huggins theory underestimates the concentration of a symmetric diblock copolymer[28] in a homopolymer melt by a factor of 5 for chain length $N = 32$ and $\epsilon = 0.15$. This corresponds to rather high incompatibilities. Figure 7 shows the absorption of a B homopolymer of chain length $N = 16$ and $N = 256$ in an A-rich homopolymer melt at $\epsilon N = 0.8$. This repulsion corresponds to $\chi N \approx 4$, *i.e.*, a temperature between the weak and strong segregation limit of the binary blend. The compositions for the different chain lengths are not identical because of the pronounced correlation hole effect in the athermal melt, which yields different values of χN even at constant ϵN. Moreover, the Flory−Huggins isotherm (eq 5.12) underestimates the concentration of the minority component for chain length $N = 16$ by a factor of 1.4 whereas the SCF is in much better agreement with the Monte Carlo data. For long chains ($N = 256$) both theories agree nicely with the simulation data. We attribute this effect to the contraction of the B polymer in the unfavorable environment.[28]

The temperature and composition dependence of the chain conformations can be partially rationalized with an interchange of energetically unfavorable intermolecular contacts with intramolecular contacts associated with the shrinking of the macromolecules. Therefore we investigate directly the number of intra- and intermolecular contacts per monomer at two-phase coexistence. The results of the Monte Carlo simulations (a) and the SCF calculations (b) are presented in Figure 8. Similar to the behavior of the single chain conformations, the difference between contacts of the minority component and the majority one decreases with N at fixed ϵN and increases proportional to ϵ for constant chain length and high incompatibilities. The Monte Carlo simulations and the SCF calculations are in good quantitative agreement.

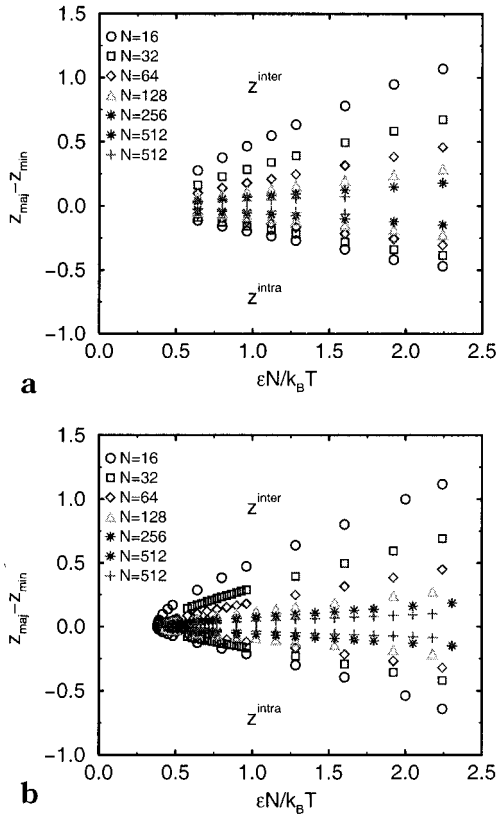

Figure 8. Inter- and intramolecular contacts per monomer in the Monte Carlo simulations (a) and the SCF calculations ($n_c = 12$) (b) at two-phase coexistence.

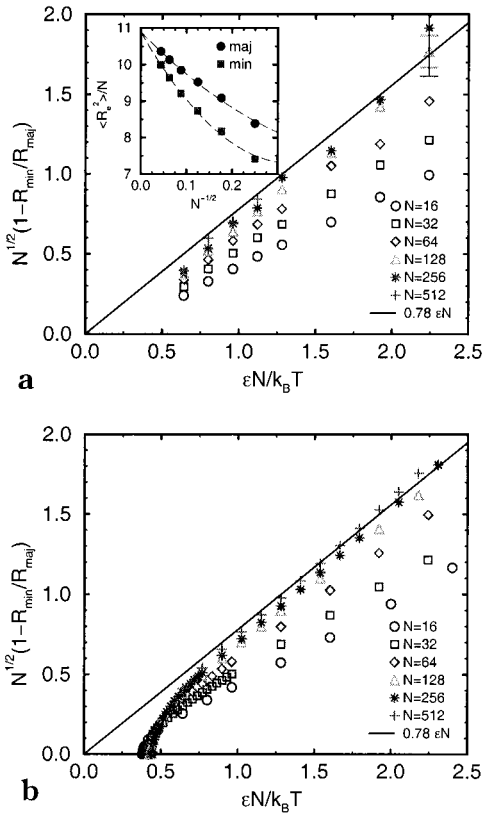

Figure 9. Shrinking of the end-to-end extension in the Monte Carlo simulations (a) and the SCF calculations ($n_c = 12$) (b) below the critical temperature. The solid line marks the expected behavior for long chain lengths. The inset in part a shows the chain length dependence of end-to-end distance of the majority and minority component at constant $\epsilon N = 0.64$. Lines are guides to the eye only.

At two-phase coexistence, there is a pronounced shrinking of the chains in the minority component for finite chain length. Using the same simple consideration than above, we expect the chain conformations to exhibit a temperature and chain length dependence of the form

$$\sqrt{N}\left(1 - \frac{\sqrt{\langle R_e^2\rangle}}{\sqrt{\langle R_e^2\rangle_0}}\right) \approx \sqrt{\frac{8}{27\pi}} b \left(\frac{dz}{dR} N\right) \epsilon N \approx 0.78 \epsilon N \quad (4.4)$$

i.e., the relative shrinking of the chain extension increases with growing incompatibility ϵN and decreases like $1/\sqrt{N}$ for large chain length N at fixed ϵN. The simulation data for the end-to-end distance and the radius of gyration are presented in Figures 9a and 10a. The relative difference in chain extensions between the minority and majority phase vanishes at the critical point (around $\epsilon N \approx 0.4$) and grows linearly with the incompatibility at higher ϵN. The simulation data show only a surprisingly slow approach of the limiting scaling behavior. Only for the longest three chain lengths does the scaling limit seems to be reached. This limiting behavior agrees well with the simple estimate above. Unfortunately it is computationally very demanding to increase the chain length or incompatibility still further, because of the increase of the relaxation times and the decrease of the relative shrinking with increasing chain length and the small fraction of chains in the minority phase for large ϵN. The largest statistical errors hence occur for large N and ϵN and are denoted by error bars in the figure for $N = 128$, 256 and $\epsilon N = 2.24$. For shorter chains and smaller incompatibility the statistical uncertainties are much smaller. The inset of Figure 9a shows the dependence of the squared end-to-end distance $\langle R^2\rangle/N$ of the minority and majority component at constant $\epsilon N = 0.64$ as a function of the chain lengths. The chain extensions of both species approaches a common value only very gradually. The corresponding results of the SCF calculations are presented in Figures 9b and 10b. They exhibit the same gradual approach to the limiting scaling behavior, and even the results for the short chain lengths agree quantitatively with the simulation data. This indicates that our SCF calculations capture most of the relevant mechanisms of the shrinking of the minority component.

There are at least two possible reasons for the pronounced correction to the limiting scaling behavior: First, the heuristic considerations above hold only in the temperature range $2 \ll 4.1\epsilon N/k_BT \approx \chi N \ll \sqrt{N}$. The first limit is set by the assumption that the blend is well segregated, *i.e.*, $\phi_{min} \ll 1$. The second limit corresponds to the requirement of small relative conformational changes which grow like $\chi N/\sqrt{N}$. Clearly, this is a relevant temperature regime in which the concentration of the minority component is small but not vanishing in the long chain length limit. For the finite chain lengths accessible to simulations, however, the temperature regime is rather small for short chains and the asymptotic behavior might be blurred by pronounced crossover effects. For very strong segregation the linear decrease of the chain dimension in terms of the scaling variable $\epsilon\sqrt{N}$ will certainly break down and there might be collapse onto a more general scaling function.

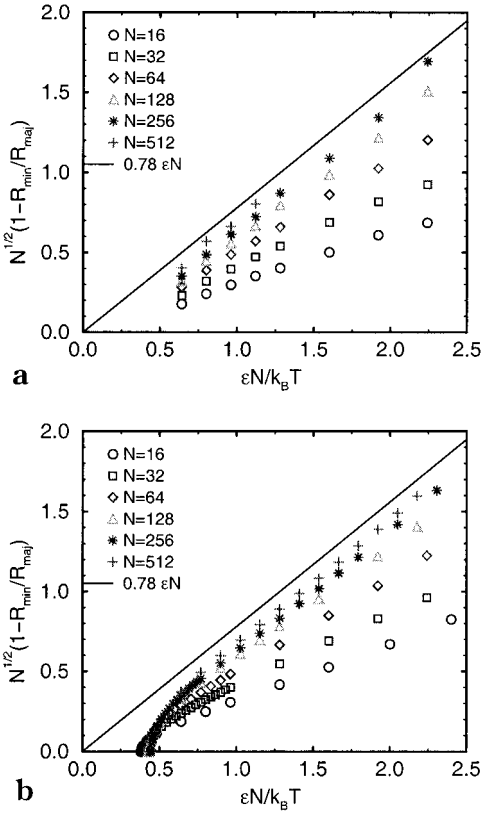

Figure 10. Shrinking of the radius of gyration in the Monte Carlo simulations (a) and the SCF calculations ($n_c = 12$) (b) at two phase coexistence. The solid line corresponds to the estimate for long chain lengths.

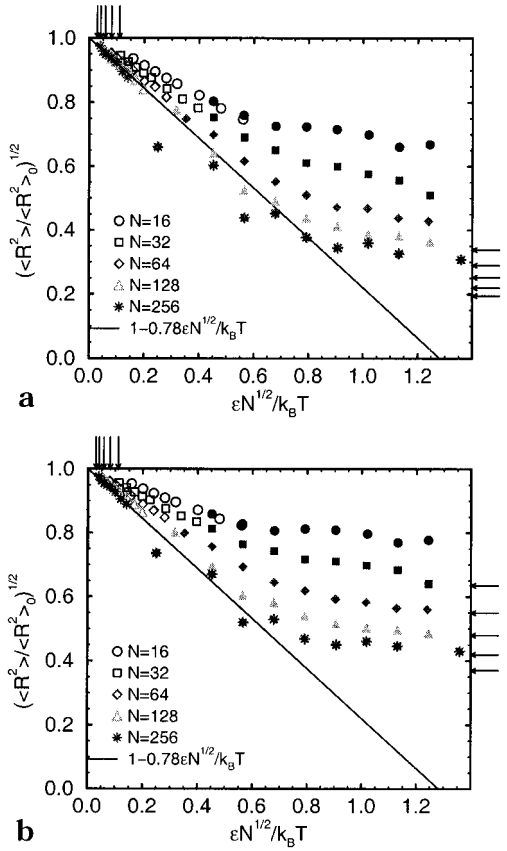

Figure 11. Shrinking of the end-to-end extension (a) and the radius of gyration (b) of the minority component in the Monte Carlo simulations. The open symbols refer to semi-grand-canonical simulations at two-phase coexistence, the filled ones correspond to canonical simulations where the concentration of the minority component is less than 1%. The arrows on the right hand side mark the ratio between the chain extension and the radius of a densely packed collapsed globule $R^3 = 3N/4\pi\Phi$ in part a or $(3/5)^{1/2}R$ in part b. The arrows on the top of the figure denote the critical temperatures of the blends.

If the chains were in a collapsed state, one might expect the free energy per chain to scale as

$$F(R) \sim \frac{N}{R^2} - \epsilon N\frac{N}{R^3} + wN\left(\frac{N}{R^3}\right)^2 \qquad (4.5)$$

at high segregation. The first term describes the conformational entropy loss of a Gaussian chain upon confinement into a cavity of size R.[64] The second contribution stems from the exchange of inter- and intramolecular contacts upon shrinking, while the third term comprises the third virial coefficient w in the expansion of the intrachain monomer density. Temperature and chain length independent prefactors in the above equation have been ignored. Minimizing this free energy with respect to the chain extension R, we obtain $R \sim (wN/\epsilon)^{1/3} \sim (w/\epsilon\sqrt{N})^{1/3}\sqrt{N}$ similar to the collapse of a chain in a poor solvent.

A second source of correction to the leading scaling behavior might be deviations from the Gaussian chain statistics upon contraction. The ratio between the end-to-end distance and the radius of a completely collapsed coil $(3/4\pi b^3\Phi\sqrt{N})^{1/3}$ decreases only very weakly with chain length. Hence, even for the longest chain length ($N = 256$) studied, the end-to-end distance exceeds the radius of the densely packed, collapsed coil only by a factor of 5. If the extension of the shrunken chain becomes comparable to the size of the completely collapsed coil it cannot shrink much further. In this case the data would not scale as a function of $\epsilon\sqrt{N}$ but would instead level off in scaling behavior earlier as the chains become shorter.

To investigate these possibilities we have extended our simulations to lower temperatures. Unfortunately, the accuracy of the SCF calculations deteriorates at very high segregation, because the conformations of the athermal reference system and the highly incompatible blend differ strongly. Hence, in our partial enumeration scheme, only the few shrunken polymers in our sample of conformations contribute to the result. Moreover, the approximation on the intercluster excluded volume interactions breaks down, because the incompatibilities for short chain lengths are close to the Θ temperature. Monte Carlo simulations in the semi-grand-canonical ensemble are also difficult because the concentration of the minority component is extremely small. Therefore we decided to study the conformations in the canonical ensemble and fix the concentration of the minority component at a value lower than 1%. Though this value exceeds the coexistence composition the small number of minority chains (1−4) in the simulation cell prevents aggregation/phase separation. The extended scaling behavior is presented in Figure 11. The linear approximation in $\epsilon\sqrt{N}$ describes the data quite well for $\epsilon\sqrt{N}/k_BT < 0.15$, and the chains exhibit a gradual contraction. For stronger segregation, however, there are systematic deviations; the linear approximation overestimates the shrinking substantially. The data collapse in the scaling plot deteriorates and the deviations set in the earlier the smaller the chain lengths. Moreover, the relative shrinking depends on whether

the end-to-end distance (a) or the radius of gyration (b) is employed. This indicates deviations from the Gaussian chain statistics and that the shrinking of the chains approaches gradually the limiting value of a partially compact chain. The limits of the perturbation treatment are marked by arrows in the figure. The radius of a compact coil is marked on the right hand side, whereas the critical incompatibilities are denoted by the arrows on the top of the figures. Hence, Monte Carlo simulations of even longer chains are necessary to determine the scaling function for large incompatibilities. The results for extremely high segregation suggest, however, that the slow approach of the asymptotic limit for the chain extensions as a function of ϵN (cf. Figures 9 and 10) can be attributed to the small ratio between the unperturbed extension and the limiting value of the coil extension in the extremely high segregation limit.

V. Discussion and Outlook

We have formulated a mean field theory for the structure and thermodynamics of a dense binary polymer blend which takes due account of the correlation between the chain conformation and the interaction energy. The self-consistent field (SCF) scheme calculates the behavior of a cluster of neighboring polymers. Intracluster interactions are treated exactly, whereas we invoke a mean field approximation for the intercluster interactions. The intercluster excluded volume is approximately incorporated via a constraint which enforces the temperature and composition independence of the average density of intercluster contacts. This is certainly only a rough *ad hoc* approximation, but the quantitative comparison with the Monte Carlo simulations reveals that this assumption yields reasonable results at least for the model studied, where the spatial range of the thermal interactions coincides with the first peak of the monomer-monomer density pair correlation function. An improvement on the quantitative predictions of the SCFT can be achieved by employing a more microscopic treatment of the excluded volume interaction along the lines of generalized Flory−Huggins theories[57] or density functional approaches.[5−7] At lower monomer densities ρ, the excluded volume effects become more important and a complete treatment of the ternary system system—polymer A, polymer B, and solvent—calls for a renormalization group analysis.[54−56] The fact that the coil size for chain length $N = 32$ and the screening length of the excluded volume interaction is comparable suggests that excluded volume effects might affect our data for small chain length.[65]

The statistical mechanics of a cluster of neighboring polymers is treated using a partial enumeration scheme which sums over a representative sample of explicit cluster conformations and all composition fluctuations inside a cluster. The scheme is applicable to extended molecules of arbitrary architecture; it describes the detailed chain conformations on all length scales and does not require a mapping onto the Gaussian chain model. Moreover, it incorporates the fluidlike structure of the athermal reference melts *via* the inter- and intramolecular contact statistics. The predictions have been compared quantitatively to Monte Carlo simulations of the bond fluctuation model without any adjustable parameter. For long chain lengths the SCFT agrees with the Flory−Huggins theory and the Monte Carlo simulations. The incompatibility parameter χ of the Flory−Huggins theory has been extracted from the intermolecular pair correlation function of the athermal reference system.[53] Hence, it already incorporates a $1/\sqrt{N}$ dependence of the number of intermolecular contacts due to the correlation hole of the athermal chain conformations. For short chain lengths, the SCFT yields corrections to the Flory−Huggins theory, which agree qualitatively with the deviations between Monte Carlo simulations and the Flory−Huggins theory. The corrections are due to nonrandom mixing and the coupling between chain conformations and the thermodynamic state. They yield corrections of relative magnitude $\chi\sqrt{N}$ to the chain conformations and the effective Flory−Huggins parameter χ_{FH}. We expect that decreasing the density will have similar effects than decreasing the chain length, because both decrease the number of neighbors a given molecule interacts with and increase the intramolecular contribution to the total energy. The heuristic considerations suggest that the density dependence of the relative chain contraction depends on $b/z^{inter}|dz/dR|$. At $\rho = 0.5/8$ this expression takes the value 1.21, whereas it increases by 21% upon reducing the density to $\rho = 0.3/8$.

For the temperature and composition dependence of the chain dimensions above the critical temperature and the chain extensions and number of inter- and intramolecular contacts in the two-phase region, we find good quantitative agreement with the Monte Carlo simulations. In agreement with intuition, the exchange of inter- and intramolecular contacts upon shrinking gives rise to a negative second virial coefficient in the expansion of the effective single chain free energy with respect to the density of its own monomers. The situation is similar to the behavior of a single chain in solution, however, the virial coefficient is of the order $\chi \sim 1/N$, and hence its effect can be treated as a perturbation.[50] This differs from the study of Weinhold *et al.*,[46] which investigates the dependence of the chain extensions on the density in polymer solutions. In polymer solutions the segmental (excluded volume) interactions v_{exc} are independent of the chain length and the interaction per polymer $v_{exc}\sqrt{N}$ does not become small for long chains. Consequently, it is difficult to treat the excluded volume interactions as a perturbation.[50] For the dense binary blend, we find pronounced effects for small chain lengths but only a mild perturbation of the Gaussian conformations for large N and not too large an incompatibility. This is qualitatively compatible with the findings of field-theoretical calculations of corrections to the mean field theory.[37,38]

The conformational properties of very long chains agree reasonably well with heuristic considerations based upon a balance between the entropy loss due to the shrinking of the chain extensions and exchange of inter- and intramolecular contacts. However, SCF calculations and Monte Carlo simulations show that this limiting scaling behavior is approached surprisingly slowly. While the scaling regime for the critical temperature $T_c \sim N$ is observed already for rather short chain lengths $N \geq 32$, the scaling of the chain extension is seen for $N \geq 128$. Simulations at high segregation suggest that the deviations from the scaling behavior are due to the small ratio between the unperturbed chain extension and the radius of a compact globule for short chain lengths. Moreover, the perturbation treatment is only reliable for very small values of the parameter $\chi\sqrt{N}$. For large chain lengths this approximation describes the behavior well, however, the rela-

tive magnitude of the effects is rather small. Hence, a detailed quantitative theory, which copes with corrections to the large N behavior, is appropriate. It should be noted that the computational demands of the SCF calculations are 2 orders of magnitude smaller than those for the Monte Carlo simulations.

Composition fluctuations on the length scale of a cluster are partially incorporated in the SCFT, but our calculations are mean field-like on greater length scales. Not surprisingly, the SCF calculations overestimate the critical temperature and cannot reproduce the flat, Ising-like shape of the binodal in the vicinity of the critical point. However, using cluster size $n_c = 14$, we reduced the relative deviation between the mean field estimate and the ("exact") Monte Carlo value of the critical temperature by one-third compared to the simple Flory−Huggins theory. Moreover, we find an upward parabolic composition dependence of the effective Flory−Huggins parameter above the critical temperature and an underestimation of the minority component density as a function of the exchange chemical potential. Again both effects become small for long chain lengths in the SCF calculations. While the SCF calculations yield quantitative agreement with the Monte Carlo simulations for the single chain conformations, the agreement for thermodynamic properties is only qualitative because nonrandom mixing effects yield corrections which are on the same order of magnitude as those due to conformational changes. Qualitatively, it is possible to distinguish between the coupling between chain conformations and energy and nonrandom mixing effects. Conformational effects are almost independent of the cluster size, whereas composition fluctuations do strongly depend on the cluster extension.

The SCF scheme can be systematically improved by increasing the cluster size n_c. However, the computational costs increase rapidly, because all 2^{n_c} chain identities are evaluated in the calculation of the single cluster partition function. If this evaluation were replaced by an importance Monte Carlo sampling, we could investigate substantially larger clusters. In this case, the scheme would be similar to a Monte Carlo simulation of a small system with "self-consistent" boundary conditions chosen as to minimize the amplitude of finite size effects. This might be useful for the simulation of systems with a small number of extended molecules, where periodic boundary conditions might systematically underestimate the number of intermolecular contacts.

The magnitude of the coupling between molecular conformations and the thermodynamic state depends strongly on the specific architecture of the molecules and their interactions. However, the qualitative features are expected to be universal. The coupling between conformations and the thermodynamic state is important for small chain length and rather high segregation. Hence, we expect it to be important also for related systems, *e.g.*, lipid−water mixtures[47] or diblock copolymers. Indeed, computer simulations,[32,33] experiments[30] and analytical theories[35,39,40] for diblock copolymers show a contraction of the individual blocks and a dumbbell-like shape of the whole molecule above the ODT. The analytical studies suggest chain length and density dependence similar to that for a binary homopolymer blend.

Having demonstrated the utility in capturing the coupling between single chain conformations and thermodynamic state, we believe that the SCF scheme might be successfully applied to study the effect of specific interactions[66] (*e.g.*, hydrogen bonds[67]) on the molecular conformations of polymers in solution. The approach can be employed to study mixtures of flexible and stiff polymers and to estimate the contributions of stiffness-dependent intermolecular interactions and steric/packing effects to the free energy of mixing. Our self-consistent field calculations can also be extended to spatially inhomogeneous systems. Potential applications comprise the study of micelles in mixtures of homopolymers and strongly asymmetric diblock copolymers or nucleation phenomena in polymeric systems.

Acknowledgment. It is a great pleasure to thank K. Binder, M. Schick, P. Janert, T. Geisinger, F. Schmid, and A. Werner for stimulating and helpful discussions. A generous allocation of computing time on the CRAY T3E of the HLRZ Juelich and the CONVEX SPP2000 of the Rechenzentrum of the university of Mainz are gratefully acknowledged. The work was financially supported by the BMBF under Grant No. 03N8008C and the DFG under Grant Bi314/17-1.

Appendix: Derivation of the SCF Equations

In this Appendix we formulate the self-consistent field theory of a system described by the multichain cluster partition function (eq 2.8). Even if the total A monomer density is spatially homogeneous, the A monomer density of a given cluster is not. Hence, we proceed by employing standard mean field techniques for spatially inhomogeneous systems: Introducing auxiliary fields, we rewrite the many cluster problem in terms of independent multichain conformations α in external, fluctuating fields $W_{A\alpha}$ and $W_{B\alpha}$.

$$Z = \int D[W_{A\alpha},W_{B\alpha},\Phi_{A\alpha},\Phi_{B\alpha},\Pi] \exp(-G[W_{A\alpha},W_{B\alpha},\Phi_{A\alpha},\Phi_{B\alpha},\Pi]/k_BT) \quad (5.1)$$

where the semi-grand-canonical free energy functional G is defined by

$$G[W_{A\alpha},W_{B\alpha},\Phi_{A\alpha},\Phi_{B\alpha},\Pi] = -k_BT\sum_\alpha \ln Q_\alpha[W_{A\alpha},W_{B\alpha}] + \sum_{\alpha\neq\beta} E^{\text{inter}}_{\text{therm}\alpha\beta}[\Phi_{A\alpha},\Phi_{B\alpha},\Phi_{A\beta},\Phi_{B\beta}] - \rho\int d\mathbf{r} \sum_\alpha\{W_{A\alpha}\Phi_{A\alpha} + W_{B\alpha}\Phi_{B\alpha}\} - \rho\int d\mathbf{r}\,\Pi(c^{\text{inter}}(\mathbf{r}) - c^{\text{inter}}_{\text{atherm}}) \quad (5.2)$$

and $Q[W_A,W_B]$ denotes the single cluster partition function in the fields W_A and W_B.

$$Q_\alpha[W_{A\alpha},W_{B\alpha}] = \int D_\alpha[\mathbf{r}]P_\alpha[\mathbf{r}] \exp\left(-\frac{E^{\text{intra}}_{\text{therm}\alpha}}{k_BT} - \frac{\rho}{k_BT}\int d\mathbf{r}\,\{W_{A\alpha}\hat{\phi}_{A\alpha} + W_{B\alpha}\hat{\phi}_{B\alpha}\} + \frac{\Delta\mu n_{A\alpha}}{k_BT}\right) \quad (5.3)$$

The functional integral for the partition function cannot be evaluated; hence, we approximate it by the saddle point of the integrand. Thus intracluster interactions are retained, but the intercluster interactions are treated in a mean field approximation. This mean field treatment of the intercluster interactions corresponds to a neglect of nonrandom mixing effects at the cluster

surfaces and results to mean field critical exponents at the critical unmixing point. If we were to neglect the intercluster interactions completely, the behavior of extremely large clusters (not accessible to our calculations) would hardy be affected, while for the smallest clusters considered, we would neglect a substantial part of the intermolecular interactions and, hence, no phase separation would occur.

The values of the collective variables, which extremize the free energy functional (eq 5.2) are denoted by lower case letters and are given by

$$\frac{\delta G}{\delta W_{A\gamma}} = -\frac{k_B T}{Q_\gamma}\frac{\delta Q_\gamma[W_{A\gamma},W_{B\gamma}]}{\delta W_{A\gamma}} - \Phi_{A\gamma} \stackrel{!}{=} 0 \Rightarrow$$

$$\phi_{A\gamma}(\mathbf{r}) = \frac{\int D_\gamma[\mathbf{r}]P_\gamma[\mathbf{r}]\hat{\phi}_{A\gamma}(\mathbf{r})\omega_\gamma[\mathbf{r}]}{\int D_\gamma[\mathbf{r}]P_\gamma[\mathbf{r}]\omega_\gamma[\mathbf{r}]} \quad \text{with}$$

$$\omega_\gamma[\mathbf{r}] = \exp\left(-\frac{E^{\text{intra}}_{\text{therm}\gamma}}{k_B T} - \frac{\rho}{k_B T}\int \mathrm{d}\mathbf{r}\,\{w_A\hat{\phi}_{A\gamma} + w_B\hat{\phi}_{B\gamma}\} + \frac{\Delta\mu n_{A\gamma}}{k_B T}\right) \quad (5.4)$$

The density of A monomers in cluster γ is the statistical average of A polymers in cluster α with respect to the multichain Boltzmann factor ω_γ. A similar expression holds for the density of B monomers. Variation with respect to $\Phi_{A\gamma}$ yields

$$\frac{\delta G}{\delta \Phi_{A\gamma}} = \sum_{\alpha\neq\beta}\frac{\delta\, E^{\text{inter}}_{\text{therm}\alpha\beta}[\Phi_{A\alpha},\Phi_{B\alpha},\Phi_{A\beta},\Phi_{B\beta}]}{\delta\Phi_{A\gamma}} - \rho W_{A\gamma} - \frac{\delta}{\delta\Phi_{A\gamma}}\rho\int \mathrm{d}\mathbf{r}\,\Pi c^{\text{inter}}(\mathbf{r}) \stackrel{!}{=} 0 \Rightarrow$$

$$w_{A\gamma}(\mathbf{r}) = -\epsilon\sum_{\beta'}\rho\int \mathrm{d}\mathbf{r}'\, v(\mathbf{r}-\mathbf{r}')[\phi_{A\beta}(\mathbf{r}') - \phi_{B\beta}(\mathbf{r}')] - \pi(\mathbf{r})\sum_{\beta'}\rho\int \mathrm{d}\mathbf{r}'\, v(\mathbf{r}-\mathbf{r}')[\phi_{A\beta}(\mathbf{r}') + \phi_{B\beta}(\mathbf{r}')] \quad (5.5)$$

where the sum over β' runs over all clusters but the cluster γ. The intercluster excluded volume interaction π is given implicitly by

$$\frac{\delta G}{\delta \Pi} = \rho(c^{\text{inter}}(r) - c^{\text{inter}}_{\text{atherm}}) \stackrel{!}{=} 0 \quad (5.6)$$

Equations 5.4−5.6 constitute a complete set of self-consistent equations for spatially inhomogeneous systems.

In the subsequent section, we apply the above equations to a spatially homogeneous situation. Hence all multichain clusters are equivalent and the cluster index α is irrelevant. The average composition of the homogeneous system is given by the cluster average (eq 2.9) with respect to the multichain Boltzmann weight (eq 2.10). Furthermore, we assume a decoupling between density and composition fluctuations for the *inter*cluster interactions:

$$w_{A\gamma}(\mathbf{r}) \approx -\epsilon(\bar{\phi}_A - \bar{\phi}_B)\sum_{\beta'}\rho\,\mathrm{d}\mathbf{r}'\, v(\mathbf{r}-\mathbf{r}')[\phi_{A\beta}(\mathbf{r}') + \phi_{B\beta}(\mathbf{r}')] - \pi\sum_{\beta'}\rho\int \mathrm{d}\mathbf{r}'\, v(\mathbf{r}-\mathbf{r}')[\phi_{A\beta}(\mathbf{r}') + \phi_{B\beta}(\mathbf{r}')] \quad (5.7)$$

Note that this approximation refers only to the contacts at the cluster boundary; hence, it becomes the better the larger the cluster. Using the number of intercluster contacts $c^{\text{inter}}(i_\gamma)$ (cf. eq 2.11) we can rewrite this expression in the following form:

$$\rho\int \mathrm{d}\mathbf{r}\,\{w_{A\gamma}(\mathbf{r})\hat{\phi}_{A\gamma}(\mathbf{r}) + w_{B\gamma}(\mathbf{r})\hat{\phi}_{B\gamma}(\mathbf{r})\} = -\epsilon(\bar{\phi}_A - \bar{\phi}_B)[\sum_{i_{A\gamma=1}}^{n_{A\gamma}} c^{\text{inter}}(i_{A\gamma}) - \sum_{i_{B\gamma=1}}^{n_{B\gamma}} c^{\text{inter}}(i_{B\gamma})] - \pi\sum_{i_\gamma=1}^{n_c} c^{\text{inter}}(i_\gamma) \quad (5.8)$$

This then yields the final expression (eq 2.10) for the Boltzmann weight of a cluster within an environment of average composition $\bar{\phi}_A$.

We solve the self-consistent field equations via a partial enumeration scheme: A large number of statistically independent multichain conformations are extracted from a Monte Carlo simulation of an athermal (*i.e.*, $\epsilon = 0$) melt. We determine the intra- and intercluster contacts $c^{\text{intra}}(i,j)$ and $c^{\text{inter}}(i)$ according to eqs 2.4 and 2.11. We employ these cluster properties to evaluate the statistical average of clusters in the external fields w_A and w_B. Thus the partial enumeration involves a summation over N_{conf} cluster conformations and all 2^{n_c} combinations of chain identities (A or B) in a given cluster, *i.e.*, we approximate the configurational integral $\int DP$ by the sum $(1/N_{\text{conf}}2^{n_c})\sum_{c=1}^{N_{\text{conf}}}\sum_{id=1}^{2^{n_c}}$. Typical values of N_{conf} range from 4096 to 32768 multichain conformations. The computational scheme is very suitable for a massively parallel computer system like the CRAY T3E.[13,47,49] We distribute the cluster conformations across the processors and each processor calculates the average over the clusters and polymer identities asigned to it. The program scales very well with the number of processors. The calculations of small clusters requires only a few seconds whereas larger clusters need substantially more CPU time.

In the limit of a single thread-like chain *i.e.*

$$n_c = 1, \quad c^{\text{intra}} = 0, \quad \text{and} \quad c^{\text{inter}}\, Nz^{\text{inter}} = \frac{\chi N k_B T}{2\epsilon} \quad (5.9)$$

the number of intercluster contacts is independent of the cluster conformation, hence, we can set $\pi = 0$. The partition function comprises two terms—an A polymer in the external field w_A and a B polymer in the field w_B. The semi-grand-canonical free energy is given by

$$\frac{G}{k_B T\, N_c} = -\ln\left\{\cosh\left(\frac{\chi N}{2}(\bar{\phi}_A - \bar{\phi}_B) + \frac{\Delta\mu}{2k_B T}\right)\right\} + \frac{\chi N}{4}(\bar{\phi}_A - \bar{\phi}_B)^2 + \frac{\Delta\mu}{2k_B T} \quad (5.10)$$

A Legendre transformation from $\Delta\mu$ to $\bar{\phi}_A$ yields the canonical free energy F.

$$F = G + \Delta\mu N_c\bar{\phi}_A = k_B T N_c\left\{\bar{\phi}_A \ln\bar{\phi}_A + \bar{\phi}_B \ln\bar{\phi}_B + \frac{\chi N}{4}(\bar{\phi}_A - \bar{\phi}_B)^2 + \ln 2\right\} \quad (5.11)$$

We recover the standard Flory−Huggins form of the free energy in the limit of single thread-like chain. The Flory−Huggins estimate for the critical temperature is

given by $kT_c/\epsilon = c^{\text{inter}} = N z^{\text{inter}}$. The semi-grand-canonical equation of state, which relates the exchange potential $\Delta\mu$ per polymer and the composition $\bar{\phi}_A$ of the mixture takes the form

$$\frac{\Delta\mu}{k_B T} = \frac{\partial F/k_B T}{\partial n_A} = \ln\left(\frac{\bar{\phi}_A}{1-\bar{\phi}_A}\right) + \chi N(2\bar{\phi}_A - 1) \quad (5.12)$$

where $n_A = \bar{\phi}_A N_c$ denotes the number of A polymers in the system. This motivates the definition of the Flory–Huggins parameter in eq 4.3. Since phase coexistence in the symmetric system occurs at $\Delta\mu = 0$, the above equation implicitly determines the binodal.

References and Notes

(1) Helfand, E.; Tagami, Y. *J. Chem. Phys.* **1972**, *56*, 3592. Helfand, E. *J. Chem. Phys.* **1975**, *62*, 999.
(2) Noolandi, J.; Hong, K. M. *Macromolecules* **1981**, *14*, 727; **1982**, *15*, 483.
(3) Shull, K. R. *Macromolecules* **1993**, *26*, 2346.
(4) Scheutjens, J. M. H. M.; Fleer, G. J. *J. Phys. Chem.* **1979**, *83*, 1619; **1979**, *84*, 178. *Macromolecules* **1985**, *18*, 1882.
(5) Tang, H.; Freed, K. F. *J. Chem. Phys.* **1992**, *96*, 8621; **1991**, *94*, 1572. McMullen, W. E.; Trache, M. *J. Chem. Phys.* **1994**, *102*, 1440. McMullen, W. E.; Freed, K. F. *J. Chem. Phys.* **1990**, *92*, 1413.
(6) Donley, J. P.; Curro, J. G.; McCoy, J. D. *J. Chem. Phys.* **1994**, *101*, 3205.
(7) Gromov, D. G.; de Pablo, J. J. *J. Chem. Phys.* **1995**, *103*, 8247. Tillman, P. A.; Rottach, D. R.; McCoy, J.; Plimpton, S. J; Curro, J. G. *J. Chem. Phys.* **1997**, *107*, 4024.
(8) Schweizer, K. S.; Curro, J. G. in *Advances in Chemical Physics*; Prigogine, I., Rice, S. A., Eds.; Wiley: New York, 1007; Vol. XCVIII.
(9) McCoy, J. D.; Nath, S. K.; Curro, J. G.; Saunders, R. S. *J. Chem. Phys.* **1998**, *108*, 3023. Nath, S. K.; McCoy, J. D.; Curro, J. G.; Saunders, R. S. *J. Chem. Phys.* **1997**, *107*, 1960.
(10) Foreman, K. W.; Freed, K. F. *J. Chem. Phys.* **1995**, *102*, 4663. Freed, K. F.; Dudowicz, J. *Macromolecules* **1996**, *29*, 625.
(11) Szleifer, I. *Current Opin. Colloid Interface Sci.* **1997**, *1*, 416. Szleifer, I.; Carignano, M. A. *Adv. Chem. Phys.* **1996**, *94*, 742.
(12) Morse, D. C.; Fredrickson, G. H. *Phys. Rev. Lett.* **1994**, *73*, 3235.
(13) Müller, M.; Werner, A. *J. Chem. Phys.* **1997**, *107*, 10764.
(14) Sariban, A.; Binder, K. *Macromolecules* **1988**, *21*, 711. *J. Chem. Phys.* **1987**, *86*, 5859. *Makromol. Chem.* **1988**, *189*, 2357.
(15) Cifra, P.; Nies, E.; Broersma, J. *Macromolecules* **1996**, *29*, 6634.
(16) Cifra, P.; Karasz, F. E.; MacKnight, W. J. *Macromolecules* **1992**, *25*, 192 and 4895.
(17) Deutsch, H.-P.; Binder, K. *Europhys. Lett.* **1992**, *18*, 667.
(18) Müller, M.; Binder, K. *J. Phys. II (Fr.)* **1996**, *6*, 187.
(19) Murat, M.; Kremer, K. *J. Chem. Phys.* **1998**, *108*, 4340.
(20) See *e.g.*: Koningsveld, R.; Kleintjens, L. A. *Macromolecules* **1971**, *4*, 637. Huggins, M. L. *J. Chem. Phys.* **1976**, *80*, 1317. Koningsveld, R.; Kleintjens, L. A.; Markert, G. *Macromolecules* **1977**, *10*, 1105.
(21) Pesci, A. I.; Freed, K. F. *J. Chem. Phys.* **1989**, *90*, 2003 and 2017.
(22) Peterson, K. A.; Stein, A. D.; Fayer, D. M. *Macromolecules* **1990**, *23*, 111.
(23) Walsh, D. J.; Higgins, J. S.; Double, C. P.; McKeown, J. G. *Polymer* **1981**, *22*, 168.
(24) Ito, H.; Russell, T. P.; Wignal, G. D. *Macromolecules* **1987**, *20*, 2213. Wignall, G. D.; Hendricks, R. W.; Koehler, W. C.; Lin, J. S.; Wai, M. P.; Thomas, E. L.; Stein, R. S. *Polymer* **1980**, *22*, 886. Wignall, G. D.; Child, H. R.; Li-Aravena, F. *Polymer* **1980**, *21*, 131.
(25) Lerman, L. S. *Proc. Natl. Acad. Sci. U.S.A.* **1971**, *68*, 1886. Laemmli, U.K. *Proc. Natl. Acad. Sci. U.S.A.* **1975**, *72*, 4288.
(26) Müller, M.; Binder, K.; Oed, W. *Faraday Trans.* **1995**, *91*, 2369.
(27) Werner, A.; Schmid, F.; Binder, K.; Müller, M. *Macromolecules* **1996**, *29*, 8241.
(28) Müller, M.; Schick, M. *J. Chem. Phys.* **1996**, *105*, 8282.
(29) Müller, M.; Schick, M. *J. Chem. Phys.* **1996**, *105*, 8885.
(30) Bartels, V. T.; Stamm, M.; Abetz, V.; Mortensen, K. *Europhys. Lett.* **1995**, *31*, 81.
(31) Maurer, W. W.; Bates, F. S.; Lodge, T. P.; Almdal, K.; Mortensen, K.; Fredrickson, G. H. *J. Chem. Phys.* **1998**, *108*, 2989.
(32) Fried, H.; Binder, K. *J. Chem. Phys.* **1991**, *94*, 8349. Binder, K.; Fried, H. *Macromolecules* **1993**, *26*, 6878.
(33) Hoffmann, A.; Sommer, J. U.; Blumen, A. *J. Chem. Phys.* **1997**, *106*, 6709.
(34) Grayce, C. J.; Schweizer, K. S. *J. Chem. Phys.* **1994**, *100*, 6846. Grayce, C. J.; Yethiraj, A.; Schweizer, K. S. *J. Chem. Phys.* **1994**, *100*, 6857.
(35) David, E. F.; Schweizer, K. S. *J. Chem. Phys.* **1994**, *100*, 7767 and 7784.
(36) Wang, Z. G. *Macromolecules* **1995**, *28*, 570.
(37) Holyst, R.; Vilgis, T. A. *J. Chem. Phys.* **1993**, 99, 4835. *Phys. Rev. E* **1994**, *50*, 2087. Brereton, M. G.; Vilgis, T. A. *J. Phys. (Fr.)* **1989**, *50*, 245.
(38) Garas, G. E.; Kosmas, M. K. *J. Chem. Phys.* **1995**, *103*, 10790; **1996**, *105*, 4789. *ibid* **1998**, *108*, 376. Kosmas, M. K. *Macromolecules* **1989**, *22*, 720.
(39) Stepanow, S. *Macromolecules* **1995**, *28*, 8233.
(40) Barrat, J.-L.; Fredrickson, G. H. *J. Chem. Phys.* **1991**, *95*, 1281.
(41) de Gennes, P. G. *Scaling concepts in polymer physics*; Cornell University Press: Ithaca, NY, 1979.
(42) Ginzburg, V. L. *Sov. Phys. Solid State* **1960**, *1*, 1824. de Gennes, P. G. *J. Phys. Lett. (Paris)* **1977**, *38*, L-441. Joanny, J. F. *J. Phys. A* **1978**, *11*, L-117. Binder, K. *Phys. Rev. A* **1984**, *29*, 341.
(43) Raos, G.; Allegra, G. *J. Chem. Phys.* **1997**, *107*, 6479; **1996**, *104*, 1626.
(44) Szleifer, I.; Widom, B. *J. Chem. Phys.* **1989**, *90*, 7524.
(45) Szleifer, I. *J. Chem. Phys.* **1990**, *92*, 6940.
(46) Weinhold, J. D.; Kumar, S. K.; Szleifer, I. *Europhys. Lett.* **1996**, *35*, 695.
(47) Müller, M.; Schick, M. *Phys. Rev. E* **1998**, *57*, 6973.
(48) Müller, M.; Schick, M. *Macromolecules* **1996**, *29*, 8900.
(49) Müller, M.; Binder, K. *Macromolecules* **1998**, *31*, 8323–8346.
(50) Freed, K. F. *Renormalization Group Theory of Macromolecules*; Wiley-Interscience: New York, 1987; p 53ff. Muthukumar, M.; Nickel, B. G. *J. Chem. Phys.* **1984**, *80*, 5839.
(51) Aguilera-Granja, F.; Kikuchi, R. *Physica A* **1992**, *182*, 331; **1992**, *189*, 81 and 108. Aguilera-Granja, F.; Kikuchi, R. *J. Phys. II (Fr.)* **1994**, *4*, 1651.
(52) Dudowicz, J.; Freed, K. F. *Macromolecules* **1991**, *24*, 5076, 5096, and 5112.
(53) Müller, M.; Binder, K. *Macromolecules* **1995**, *28*, 1825.
(54) Nose, T. *J. Phys. (Fr.)* **1986**, *47*, 517.
(55) Joanny, J.-F.; Leibler, L.; Ball, R. *J. Chem. Phys.* **1984**, *81*, 4640.
(56) Schaefer, L.; Kappeler, C. *J. Chem. Phys.* **1993**, *99*, 6135. Schaefer, L.; Kappeler, C. *J. Phys. (Fr.)* **1985**, *46*, 1853.
(57) Hertanto, A.; Dickman, R. *J. Chem. Phys.* **1988**, *89*, 7577. Deutsch, H.-P.; Dickman, R. *J. Chem. Phys.* **1990**, *93*, 8963. Foreman, K. W.; Freed, K. F. *J. Chem. Phys.* **1995**, *102*, 4663.
(58) Carmesin, I.; Kremer, K. Macromolecules **1988**, *21*, 2819. Deutsch, H.-P.; Binder, K. *J. Chem. Phys.* **1991**, *94*, 2294.
(59) Paul, W.; Binder, K.; Heermann, D. W.; Kremer, K. *J. Chem. Phys.* **1991**, *95*, 7726.
(60) Müller, M. *Macromolecules* **1995**, *28*, 6556.
(61) The number of self-contacts in a single chain scales as $Nz^{\text{inter}} = 2.48N - 2.41\sqrt{N} - 0.52$. The linear term stems from the contribution of neighbors along the chain. Cf. also: Müller, S.; Schaefer, L.; *Eur. Phys. J.* **1998**, *B2*, 351.
(62) Huggins, M. L. *J. Chem. Phys.* **1941**, *9*, 440. Flory, P. J. *J. Chem. Phys.* **1941**, *9*, 660.
(63) Schweizer, K. S.; Yethiraj, A. *J. Chem. Phys.* **1993**, *98*, 9053. Yethiraj, A.; Schweizer, K. S. *J. Chem. Phys.* **1993**, *98*, 9080.
(64) Daoud, M.; de Gennes, P. G. *J. Phys. (Fr.)* **1977**, *38*, 85.
(65) Müller, M.; Baschnagel, J.; Binder, K. Manuscript in preparation.
(66) Young, A. M.; Higgins, J. S.; Peiffer, D. G; Rennie, A. R. *Polymer* **1996**, *37*, 2125.
(67) Painter, P. C.; Berg, L. P.; Veytsman, B.; Coleman, M. M. *Macromolecules* **1997**, *30*, 7529. Zhou, C.; Hobbie, E. K.; Bauer, B. J.; Sung, L.; Jiang, M.; Han, C. C. Macromolecules **1998**, *31*, 1937.

MA9807973